International Journal of Multidisciplinary Research and Bulletin
ISSN 3108-1428
Volume 5 Issue 4 (July – Aug) 2026

Histomorphology and histomorphometry changes in the hippocampal regions of kaolin-induced hydrocephalic adult rats

Blessing Oluwakemi Abe[1*], Luke Gbenga Ogungbe[1], David Temidayo Ovioke[1], Oyinlademi Modupe Awosanya[1], Aishat Yusuf Musa[1], Aishat Eniola Adelakun[1], Temidayo Mercy Adediran[1], Chidinma Jennifer Awogu[1], Olugbenga Olawole Olayinka[2]

*Correspondence: Blessing Oluwakemi Abe

[1]Department of Anatomy, Lead City University, Ibadan, Oyo State, Nigeria.

[2]Department of Anatomy, Babcock University, Ilishan, Remo, Ogun State, Nigeria.

Article History

Received: 31 July 2026 | Accepted: 14 Aug 2026 | Published: 16 Aug 2026

DOI: 10.5281/zenodo.21967557

ABSTRACT

Background: The pathological state known as hydrocephalus arises when cerebrospinal fluid builds up abnormally, causing the ventricles to expand and triggering a steady decline in neuronal health. To replicate this neurological anomaly in laboratory settings, researchers frequently administer kaolin—a type of aluminum silicate—directly into the cisterna magna. Despite its widespread application, there remains a noticeable gap in understanding how this experimental model specifically alters the microscopic anatomy and cellular metrics of the hippocampus, especially concerning the dentate gyrus. Consequently, the current investigation aimed to meticulously evaluate the morphological and morphometric shifts occurring within the adult rat hippocampus following sterile kaolin exposure.

Methods: The experiment utilized mature male rats, initiating hydrocephalus via an intracisternal injection containing 0.04 mL of a 250 mg/mL kaolin mixture for the experimental cohort (n=6), whereas the control rats (n=6) underwent a sham operation. Throughout the four-week observation window, the animals' body masses were recorded on a weekly basis. At the conclusion of this period, intracardiac perfusion was performed to euthanize the rats and safely extract their brain tissue. To accurately evaluate the extent of neuronal degradation, the harvested specimens were subjected to Cresyl violet staining protocols. Subsequent data evaluation was executed utilizing ImageJ alongside GraphPad Prism version 8.

Results: Statistical evaluations revealed a pronounced decrease in the overall body mass of the kaolin injected rats when juxtaposed with the sham-operated group ($p<0.0001$). Microscopic evaluation of the

Cresyl violet-dyed hippocampal sections highlighted a severe disruption in the layered cellular architecture within the hydrocephalic specimens, standing in stark contrast to the preserved structure found in healthy controls. Furthermore, quantitative analysis demonstrated that the pyknotic indices (PI) specific to the CA3 and dentate gyrus zones were remarkably elevated in the 250 mg/mL kaolin group.

Conclusion: The induction of hydrocephalus via kaolin leads to substantial deterioration of the hippocampus. This neurodegeneration manifests physically through the breakdown of cytoarchitecture, a noticeable drop in healthy neurons, and a surge in pyknotic (dying) cells. Ultimately, these morphological outcomes highlight the destructive impact of ventricular enlargement on hippocampal health, validating this specific animal model for observing structural brain damage.

Keywords: aluminum silicate induction, ventricular enlargement, pyramidal cells, neuronal death index, hippocampal anatomy.

1.0 INTRODUCTION

Recognized globally as a prevalent neurological condition, hydrocephalus is fundamentally driven by a disproportionate pooling of cerebrospinal fluid (CSF) inside the brain's ventricular cavities. This localized fluid retention invariably forces the ventricles to dilate, which consequently drives up intracranial pressure and paves the way for severe, often irreversible, cerebral impairment (Zhang et al., 2024; Wang et al., 2025).

The underlying mechanisms by which hydrocephalus inflicts structural brain damage are multifaceted. Primarily, the surge in intracranial pressure physically squeezes the surrounding brain parenchyma. Such mechanical compression inherently constricts local vascular networks, severely hindering cerebral blood perfusion. This lack of adequate blood supply instigates localized ischemia, culminating directly in neuronal trauma and subsequent cell death (Del Bigio, 2001; Pinto et al., 2025). Furthermore, as the condition progresses, the brain tissue suffers from relentless mechanical stretching and sustained tension, which is often compounded by an inability to efficiently clear metabolic toxins from the localized environment (Del Bigio, 2004; McAllister, 2012).

In experimental neuroscience, a highly regarded technique for mimicking this condition in living subjects involves the subarachnoid injection of kaolin, a biologically unreactive clay compound (Khan et al., 2008). Introducing this suspension provokes an intense inflammatory cascade specifically localized at the drainage pathways of the fourth ventricle. This initial acute reaction transitions rapidly into persistent meningeal scarring and fibrous tissue formation, effectively obstructing the natural transit of CSF and guaranteeing subsequent ventricular ballooning (Kang et al., 2013; Dewan et al., 2016). Extensive documentation exists regarding the neuroinflammatory fallout triggered by this obstruction across varying developmental stages in animal models, spanning from neonatal (Khan et

al., 2006; Warf et al., 2010) and juvenile subjects (Olapade et al., 2012; Abe et al., 2024) to fully mature adults (Ge et al., 2021; Femi-Akinlosotu et al., 2024).

Despite these extensive investigations, a distinct void persists in the scientific literature regarding the precise quantitative alterations impacting the pyramidal neurons across different hippocampal sectors, with a particular scarcity of data regarding the dentate gyrus in adult Wistar rats subjected to sterile kaolin. To bridge this empirical gap, the present investigation was conceptualized to comprehensively analyze both the morphological presentation and the cellular metrics of pyramidal neurons situated within the CA1, CA3, and dentate gyrus territories of mature Wistar rats, specifically ensuing the administration of a 250 mg/mL kaolin formulation.

2.0 MATERIAL AND METHODS

2.1 Experimental Animals

For this investigation, twelve fully grown male Wistar rats, weighing strictly between 215g and 230g, were mobilized. Procurement of these specimens was facilitated through a recognized animal breeding center situated in close proximity to Lead City University. The animals were maintained in aerated plastic enclosures, strictly adhering to standard laboratory protocols which included a controlled 12-hour alternating light and dark schedule. These housing arrangements were managed by the Central Animal House, a facility operated by the Faculty of Basic Medical and Health Sciences at Lead City University in Ibadan, Nigeria. The rodents were distributed equally into two distinct cohorts: a primary experimental group containing six rats, alongside a corresponding control group of six. Before initiating any invasive procedures, a 14-day acclimatization phase was strictly observed, during which the animals were granted unrestricted access to purified drinking water and standard commercial rodent nourishment.

Prior to the study's kickoff, the Research Ethics Committee of the Human Anatomy Department at Lead City University formally reviewed and approved the experimental blueprint (Approval designation: LCU/REC/ANA/047/25). Every protocol involving the animals strictly paralleled internationally recognized directives ensuring the humane and ethical treatment of laboratory animals.

2.3 Experimental Design and Induction of Hydrocephalus

Rats designated for the hydrocephalic arm of the study were sedated utilizing a precisely calculated intramuscular dosage of a ketamine-xylazine compound administered at 90/10 mg/kg. To precipitate the hydrocephalic state, a singular intracisternal delivery of 0.04 mL of a sterile kaolin preparation

(formulated at 250 mg/mL) was executed. This technique closely mirrored the established protocols previously outlined by Ayannuga and Naicker (2017), alongside Abe et al. (2024). Conversely, the control group was subjected to an identical procedural environment, minus the actual kaolin injection, effectively serving as a sham operation. Post-anesthesia, every rat underwent rigorous continuous monitoring for a span of 30 to 60 minutes to rapidly identify any immediate procedural side effects or potential fatalities before being safely transitioned back to their respective enclosures. To track physiological trajectories, the body mass of every participant was continuously logged on a weekly basis spanning the entire four-week duration of the trial.

2.4 Tissue collection and preparation

Upon reaching the conclusion of the four-week post-induction timeframe, profound anesthesia was administered to the animals prior to transcardial perfusion, utilizing a 10% neutral buffered formalin solution as the primary fixative. Following this, the cranial vaults were opened, and the brains were meticulously extracted and submerged entirely in the identical fixative solution for an additional 48hour window, thereby guaranteeing absolute cellular preservation. Subsequent to this fixation phase, the brain tissues were carefully sectioned transversely at the anatomical level of the optic chiasm and subjected to conventional histological processing regimens. This sequence began with progressive dehydration utilizing ascending ethanol gradients ranging from 70% to 100%. Clearing was achieved through dual immersions in xylene, which was immediately followed by a four-hour infiltration phase utilizing liquid paraffin wax maintained at an exact temperature of 60°C. The processed specimens were then cast into solid paraffin blocks, permitted to chill overnight in a 4°C environment, and finally sliced into microtome sections exactly 5 µm in thickness.

For the staining procedure, these paraffin ribbons were first cleared of wax by passing them through two to three separate xylene baths lasting 10 minutes a piece. Rehydration was accomplished via a reverse sequence of declining ethanol concentrations, culminating in rinses with standard tap water and then purified distilled water. The actual staining involved applying a 0.1% Cresyl violet solution, combined with an incubation phase inside an oven regulated between 37°C and 50°C. Residual dye was washed away with a rapid distilled water rinse, and the sections were visually differentiated using a 95% ethanol solution for roughly two to three minutes. Final steps included absolute alcohol dehydration, xylene clearing, and secure mounting. Microscopic validation was performed to ensure optimal stain quality. Visual data was permanently recorded utilizing a digital light microscope manufactured by Leica. For quantitative metrics, the total count of healthy versus pyknotic (degenerating) neurons was tallied at a magnification of X40. The calculation of the pyknotic index strictly adhered to the mathematical framework established by Taveira et al. (2013) and subsequently utilized by Femi-Akinlosotu et al. (2024), utilizing the equation:

Pyknotic Index (%) = (Number of pyknotic neurons ÷ Total number of neurons) × 100

2.5 Statistical and Data Analysis

All numerical data originating from the cellular counts and mass measurements were mathematically articulated as the mean value ± the standard error of the mean (SEM). To ascertain statistical variances between the designated groups, a two-way analysis of variance (ANOVA) was deployed for the body weight metrics, while an unpaired (independent-samples) t-test was applied to the neuronal count data. These primary evaluations were subsequently reinforced by applying a Bonferroni post hoc verification utilizing the GraphPad Prism software suite (version 8.4.3.686, engineered for Windows by developers in San Diego, CA, USA). Any resulting probability value ($p < 0.05$) was formally recognized as statistically significant.

3.0 RESULTS

3.1 Weekly Body weight

Observations regarding mass revealed a continuous upward growth trajectory for the sham-operated control rats across the entire study timeline. Conversely, the experimental rats burdened with hydrocephalus experienced a distinct reduction in overall body weight during the initial seven days following the kaolin induction. It was only at the onset of the second week that their physiological decline arrested; from that juncture, they began to incrementally accumulate mass until the experiment concluded. Graphical representations of this weekly data (Figure 1) starkly highlighted that despite their late recovery, the final weights of the afflicted rats remained profoundly and significantly suppressed when contrasted against the robust growth of the control population ($p<0.0001$).

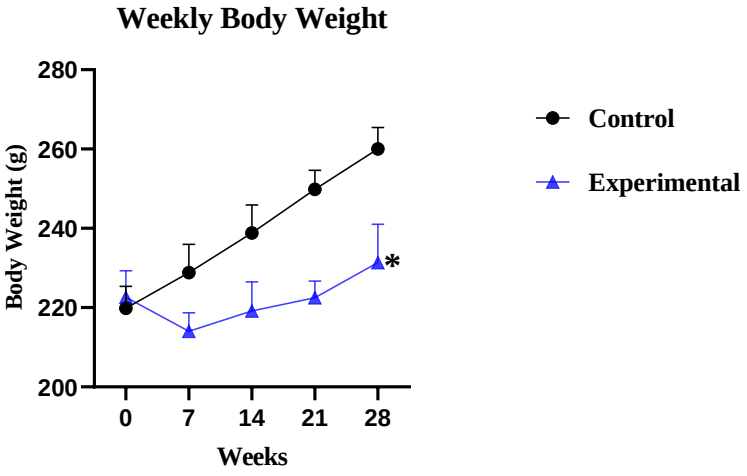

Figure 1: A line graph of the weekly body weight of control and hydrocephalic rat, showing that body weight of hydrocephalic rats is significantly higher than the control (*) ($p<0.0001$).

3.2 Histological analysis of hippocampal regions

Detailed microscopic scrutiny of the Cresyl violet-treated brain slices focusing on the CA1, CA3, and dentate gyrus regions uncovered a catastrophic breakdown of the standard laminal cytoarchitecture. Specifically, the pyramidal neurons residing in these zones within the hydrocephalic rats were severely disorganized. This structural chaos was intimately accompanied by visibly enlarged lateral ventricles, presenting a stark departure from the highly organized cellular layering witnessed in the untreated controls (Figure 2).

Delving deeper into the specific micro-anatomy of the CA3 and dentate gyrus sectors of the afflicted animals, the visual evidence presented a landscape heavily populated by abnormal, darkly stained, and physically compressed neuronal bodies displaying vacuolization—a classic hallmark of pyknosis. Healthy, viable pyramidal cells in these specific regions were alarmingly sparse. This pathological presentation stood in direct opposition to the histology of the control group, wherein the CA3 and dentate gyrus tissues were dominated by a dense population of plump, rounded, and highly active pyramidal neurons boasting clearly defined central nuclei, interspersed with only a negligible fraction of shrunken, darkened cells. Quantitative translations of these visual findings further cemented the narrative; the calculated pyknotic indices for both the CA3 and dentate gyrus territories within the experimental group were elevated to a degree of statistical significance when matched against the controls (both CA3 and Dentate Gyrus yielded $p<0.0001$) (Figures 3 and 4).

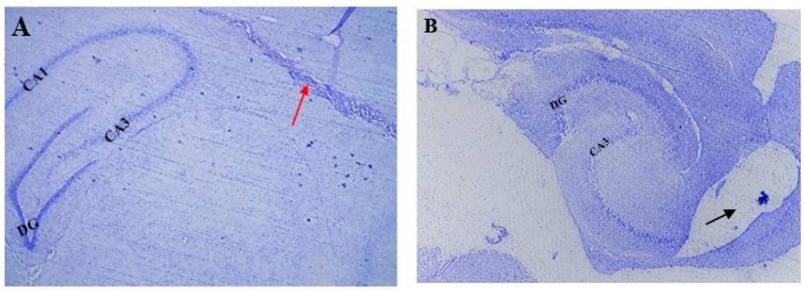

Figure 2: Photomicrographs of Cresyl violet-stained hippocampal regions (CA3, dentate gyrus) showed severely disorganized laminal cytoarchitecture of hydrocephalic rats with dilated lateral ventricles (black arrow) compared to control. NOTE; Only the CA3 and Dentate Gyrus regions of the hydrocephalic group could be identified due to the severely disorganized cytoarchitecture of the hippocampus.

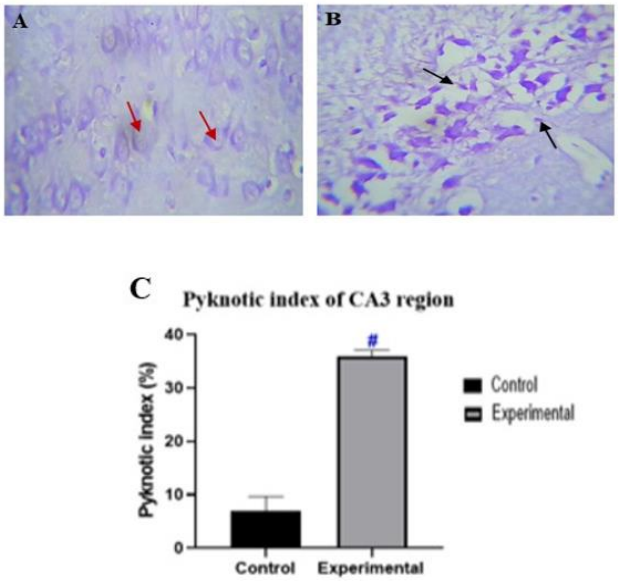

Figure 3: Photomicrographs of Cresyl violet stained CA3 of control (A) and (B) 250mg/ml of kaolin induced hydrocephalic rat, showing abundant pyknotic pyramidal neurons (black arrow) in CA3 region of the hippocampus compared to the control. (C) Bar chat of the pyknotic index of both groups, showing that the pyknotic index of CA3 of hydrocephalic rats is significantly higher than the control (#) ($p<0.0001$) (Scale bar: 50µm).

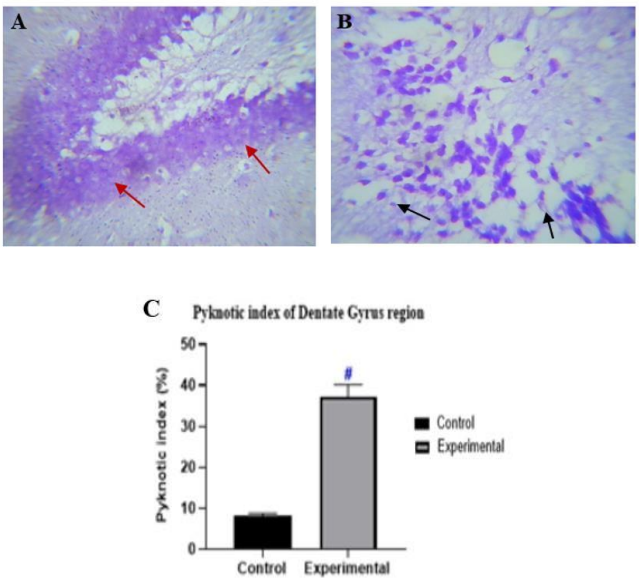

Figure 4: Photomicrographs of Cresyl violet-stained dentate gyrus of control (A) & (B) 250mg/ml of kaolin induced hydrocephalic rats showing abundant pyknotic pyramidal neurons (black arrow) in the dentate gyrus region of the hippocampus compared to the control. (C) Bar chat of the pyknotic index of both groups, showing that the pyknotic index of Dentate Gyrus of hydrocephalic rats is significantly higher than the control (#) ($p<0.0001$) (Scale bar: 50µm).

4.0 DISCUSSION

Within the realm of experimental neurology, numerous animal paradigms have been engineered across various species utilizing diverse chemical and mechanical agents to simulate hydrocephalus. Among these, the direct intracisternal delivery of kaolin remains the preeminent and most globally accepted methodology. Deploying kaolin in adult Wistar rats yields a highly consistent and replicable biological model, allowing researchers to thoroughly dissect the underlying pathophysiological mechanisms of the disease (Del Bigio, 2010; Di Curzio, 2018). This specific investigation directed its focus toward analyzing how this kaolin-driven hydrocephalus dictates structural changes in the CA1, CA3, and dentate gyrus regions of the hippocampus in mature male Wistar rats.

A primary physiological indicator observed during this study was the undeniable correlation between hydrocephalic induction and hampered body mass retention in the adult rats. Although the experimental cohort did eventually display an upward weight trend in the latter stages of the timeline, their total mass acquisition fell significantly short of the healthy benchmarks set by the control rats. This phenomenon of stymied physical growth or active weight regression is a heavily documented and anticipated clinical feature in animal models suffering from induced hydrocephalus (Liu et al., 2021; Femi-Akinlosotu et al., 2024; Abe et al., 2024).

The definitive anatomical signature of hydrocephalus is the pathological expansion of the brain's ventricular cavities. Aligning perfectly with this diagnostic criterion, the current findings verified that every single rat subjected to the kaolin treatment developed significantly dilated lateral ventricles when visually compared to the normal anatomical dimensions of the controls. This physical alteration directly mirrors the previous documentations provided by researchers such as López et al. (2009), Femi-Akinlosotu et al. (2024), and Abe et al. (2024).

Upon microscopic evaluation, the tissue sections treated with Cresyl Violet exposed a drastic and severe disarray in the spatial arrangement of the pyramidal layer spanning the CA1, CA3, and dentate gyrus. Currently, the scientific library holds limited comprehensive data regarding precisely how fluid accumulation dictates the physical fate of these specific hippocampal sub-regions. Previously, Shokunbi and colleagues (2020) documented a relatively mild structural disruption strictly within the CA1 pyramidal layer of mice following kaolin exposure. In stark contrast to the severe findings of the present study, recent work by Femi-Akinlosotu et al. (2024) suggested that the underlying cytoarchitecture across the CA1, CA3, and dentate gyrus managed to remain largely intact and organized in their respective murine models.

Furthermore, the cellular layout observed in the afflicted rats from this study was characterized by noticeably clumsy, heavily clustered, and physically squashed pyramidal neurons, which blatantly contradicted the clear, sharply defined cellular boundaries characteristic of the control samples.

This specific morphological degradation aligns closely with the observations published by Shokunbi et al. (2020) and Femi-Akinlosotu et al. (2024), both of whom detailed an abnormal disarray in pyramidal layering combined with unusual chromatin clumping inside the hippocampi of their adult mice. When inspecting the surrounding nerve fiber network of the CA3 and dentate gyrus, a striking abundance of darkly stained, shriveled neurons was visually apparent in the experimental animals. Meanwhile, the identical neurological zones in the control rats showcased thriving populations of large, metabolically active pyramidal bodies, with pyknotic remnants being exceptionally rare. These stark morphological divergences have been independently corroborated by the findings of Taveira et al. (2012) and Akinlosotu et al. (2024). Consequently, the empirical data gathered here undeniably reinforces the premise that kaolin-induced hydrocephalus aggressively deteriorates the microscopic morphology of hippocampal pyramidal cells in mature rats.

Quantitative evaluation further revealed that the pyknotic indices derived from both the CA3 and dentate gyrus of the treated rats eclipsed those of the control group by a significant margin. In a related context, Shokunbi et al. (2020) previously noted a statistically meaningful spike in the pyknotic index strictly within the CA1 zone examined one-week post-induction. However, in that same study, they found no significant statistical divergence in the CA3 pyknotic index between their experimental and control groups. Adding to the complexity of the literature, López et al. (2009) asserted that hydrocephalic mice experienced no outright, widespread neuronal depletion within the hippocampus, despite acknowledging the localized presence of some pyknotic cells.

Exploring the literature further, Femi-Akinlosotu et al. (2024) reported that the dentate gyrus pyknotic index in healthy controls was considerably lower than that seen in mature mice injected with a 250 mg/mL kaolin dose. Interestingly, their statistical analysis failed to find a significant difference in the death indices of the CA1 and CA3 regions between their treated and untreated animals. It is imperative to highlight that in the present investigation, the sheer magnitude of the cellular disorganization wrought upon the hippocampus by the hydrocephalic state was so extreme that only the CA3 and dentate gyrus territories retained enough structural integrity to be reliably identified and mathematically quantified.

5.0 CONCLUSION

To date, the scientific community has been provided with a surprisingly sparse volume of information detailing how kaolin-induced hydrocephalus dictates the fate of the dentate gyrus, as the overwhelming majority of historical research has tunneled its focus almost exclusively onto the CA1 and CA3 territories. Striving to rectify this, the current research initiative undertook a rigorous approach—combining qualitative morphological observations with hard quantitative metrics—to fully

map the pathological impact across all three primary hippocampal zones utilizing Cresyl violet staining techniques.

The conclusive data extracted from this endeavor explicitly demonstrates that the onset of hydrocephalus fundamentally shatters the normal, organized cellular layering inherent to the CA1, CA3, and dentate gyrus. Beyond mere structural disarray, the condition actively triggers profound and measurable destruction of the pyramidal neurons residing within these vital memory centers following the intracisternal delivery of kaolin.

Moving forward, it is strongly advocated that future experimental designs incorporate a broader spectrum of advanced, highly specific confirmatory staining techniques. Utilizing more sophisticated assays will be paramount in thoroughly corroborating and further detailing the extensive anatomical damage inflicted upon the hippocampal regions by this debilitating neurological condition.

Article Publication Details
This article is published in the **International Journal of Multidisciplinary Research and Bulletin**, ISSN 3108-1428 (Online). In Volume 5 Issue 4 (July – Aug) 2026.
The journal is published and managed by **IRPG**.

Acknowledgements
The primary investigators extend their sincere gratitude to the administration of Lead City University for graciously providing full access to their state-of-the-art laboratory facilities, without which this research would not have been possible. Furthermore, a special note of appreciation is directed toward Mr. Ajao Ridwan, the dedicated Laboratory Technologist stationed at the Human Anatomy Department of Lead City University. His hands-on expertise and continuous assistance throughout the practical bench work phases were absolutely invaluable.

Authors' contributions
B.O.A. led the conceptualization phase. Methodology design was a collaborative effort between B.O.A. and L.G.O. Formal data analysis was executed directly by B.O.A. Project supervision was jointly handled by B.O.A. and L.G.O. The administrative oversight of the project was managed by B.O.A., L.G.O., and D.T.O. The initial drafting, writing, resource gathering, and data curation were collectively undertaken by D.T.O., O.M.A., A.Y.M., A.E.A., T.M.A., C.J.A., and O.O.O. Prior to submission, the final manuscript was thoroughly read, and its publication was unanimously approved by all contributing authors.

Funding
The authors declare that no funding was received for this work.

Data availability

No datasets were generated or analyzed during the current study.

Declarations

Ethics approval and consent to participate

The author(s) declare that it is not applicable.

Consent for publication

The author(s) declare that this is not applicable.

Competing interests

The author(s) declare that they have no competing interests.

References

1. Zhang, M., Hu, X., & Wang, L. (2024). A review of cerebrospinal fluid circulation and the pathogenesis of congenital hydrocephalus. *Neurochemical Research*, 49(5), 1123-1136.
2. Wang, H., Chen, X., You, C., Wu, K., & Sun, T. (2025). Navigating challenges in hydrocephalus following intraventricular hemorrhage: a comprehensive review of current evidence. *Frontiers in Neurology*, 16, 1630286.
3. Del Bigio, M. R. (2001). Pathophysiologic consequences of hydrocephalus. *Neurosurgery Clinics of North America*, 12(4), 639-649.
4. Pinto, V. L., & Adeyinka, A. (2025). Increased Intracranial Pressure. In *StatPearls*. Treasure Island (FL): StatPearls Publishing. Retrieved from https://www.ncbi.nlm.nih.gov/books/NBK482119
5. Del Bigio, M. R. (2004). Cellular damage and prevention in childhood hydrocephalus. *Brain Pathology*, 14(3), 317-324.
6. McAllister, J. P. (2012). Pathophysiology of congenital and neonatal hydrocephalus. *Seminars in Fetal and Neonatal Medicine*, 17(5), 285–294.
7. Khan, O. H. (2008). Neonatal and juvenile rats with kaolin-induced hydrocephalus: pathogenesis and treatments.
8. Kang, K., Yoon, U., Lee, J. M., & Lee, H. W. (2013). Idiopathic normal-pressure hydrocephalus, cortical thinning, and the cerebrospinal fluid tap test. *Journal of the Neurological Sciences*, 334(12), 55-62.
9. Dewan, M. C., Rattani, A., Mekary, R., Glancz, L. J., Yunusa, I., Baticulon, R. E., ... & Warf, B. C. (2018). Global hydrocephalus epidemiology and incidence: systematic review and meta-analysis. *Journal of Neurosurgery*, 130(4), 1065-1079.

10. Khan, O. H., Enno, T. L., & Del Bigio, M. R. (2006). Brain damage in neonatal rats following kaolin induction of hydrocephalus. *Experimental Neurology*, 200, 311-320.
11. Warf, B. C. (2010). East African Neurosurgical Research Collaboration. Pediatric hydrocephalus in East Africa: prevalence, causes, treatments, and strategies for the future. *World Neurosurgery*, 73(4), 296-300.
12. Olopade, F. E., Shokunbi, M. T., & Sirén, A. L. (2012). The relationship between ventricular dilatation, neuropathological and neurobehavioural changes in hydrocephalic rats. *Fluids and Barriers of the CNS*, 9, 1-10.
13. Abe, B. O., Ogungbe, L. G., Kehinde, O. F., Ayoola, M. A., Olutunde, O. M., Agboola, O. O., ... & Adesanya, E. (2024). Dose-dependent alterations in dorso-ventral and antero-posterior ventricular diameters of the brain in juvenile Wistar rats following intracisternal kaolin injection. *FUOYE Journal of Biomedical Research*, 1, 114–120.
14. Ge, Y., Lai, Q., Wang, W., & Xu, X. (2021). Delayed transient obstructive hydrocephalus after cerebral aneurysm rupture. A case report. *Medicine (Baltimore)*, 100, 19-22.
15. Femi-Akinlosotu, O. M., Olopade, F. E., Abe, B. O., & Shokunbi, M. T. (2024). Ventricular enlargement, neurodegeneration and mortality rates in experimentally induced hydrocephalic adult mice using varying concentrations of intracisternal kaolin suspension. *Archives of Basic and Applied Medicine*, 12, 1.
16. Ayannuga, O. A., & Naicker, T. (2017). Cortical Oligodendrocytes in Kaolin-Induced Hydrocephalus in Wistar Rat: Impact of Degree and Duration of Ventriculomegaly. *Annals of Neurosciences*, 24, 164–172.
17. Taveira, K. V., Carraro, K. T., Catalão, C. H., & Lopes, L. S. (2013). Morphological and morphometric analysis of the hippocampus in Wistar rats with experimental hydrocephalus. *Pediatric Neurosurgery*, 48, 163-167.
18. Del Bigio, M. R. (2010). Neuropathology and structural changes in hydrocephalus. *Developmental Disabilities Research Reviews*, 16, 16-22.
19. Di Curzio, D. L. (2018). Animal Models of Hydrocephalus. *Journal of Modern Neurosurgery*, 8, 57-71.
20. Liu, C., Chen, Y., Cui, W., Cao, Y., Zhao, L., Wang, H., ... & Zhou, L. (2021). Inhibition of neuronal necroptosis in kaolin-induced hydrocephalus. *Cell Proliferation*, 54, e13108.
21. Lopes, S., Slobodian, I., & Del Bigio, M. R. (2009). Characterization of juvenile and young adult mice following induction of hydrocephalus with kaolin. *Experimental Neurology*, 219, 187-196.

22. Shokunbi, M. T., Olopade, F. E., Femi-Akinlosotu, O. M., & Ajiboye, E. O. (2020). Pyramidal cell morphology and cell death in the hippocampus of adult mice with experimentally induced hydrocephalus. *Nigerian Journal of Paediatrics*, 47, 298-304.